

See discussions, stats, and author profiles for this publication at: <https://www.researchgate.net/publication/273468504>

Inside Cover: Pulse Radiolysis and Ultra-High-Performance Liquid Chromatography/High-Resolution Mass Spectrometry Studies on the Reactions of the Carbonate Radical with Vitamin B 1...

ARTICLE *in* CHEMISTRY - A EUROPEAN JOURNAL · MARCH 2015

Impact Factor: 5.73 · DOI: 10.1002/chem.201406269 · Source: PubMed

CITATION

1

READS

30

4 AUTHORS, INCLUDING:



[Rohan S Dassanayake](#)

Texas Tech University

9 PUBLICATIONS 16 CITATIONS

SEE PROFILE



[Diane E Cabelli](#)

Brookhaven National Laboratory

99 PUBLICATIONS 3,125 CITATIONS

SEE PROFILE

Analytical Chemistry | Hot Paper |



Pulse Radiolysis and Ultra-High-Performance Liquid Chromatography/High-Resolution Mass Spectrometry Studies on the Reactions of the Carbonate Radical with Vitamin B₁₂ Derivatives

Rohan S. Dassanayake,^[a] Jacob T. Shelley,^[a] Diane E. Cabelli,^{*,[b]} and Nicola E. Brasch^{*,[c]}

Abstract: The reactions of the carbonate radical anion ($\text{CO}_3^{\cdot-}$) with vitamin B₁₂ derivatives were studied by pulse radiolysis. The carbonate radical anion directly oxidizes the metal center of cob(II)alamin quantitatively to give hydroxycobalamin, with a bimolecular rate constant of $2.0 \times 10^9 \text{ M}^{-1} \text{ s}^{-1}$. The reaction of $\text{CO}_3^{\cdot-}$ with hydroxycobalamin proceeds in two steps. The second-order rate constant for the first reaction is $4.3 \times 10^8 \text{ M}^{-1} \text{ s}^{-1}$. The rate of the second reaction is independent of the hydroxycobalamin concentration and is approximately $3.0 \times 10^3 \text{ s}^{-1}$. Evidence for formation of corrinoid complexes differing from cobalamin by the abstraction of two or four hydrogen atoms from the corrin macrocycle and lactone ring formation has been obtained by ultra-high-performance liquid chromatography/high-resolution mass

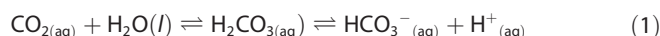
spectrometry (UHPLC/HRMS). A mechanism is proposed in which abstraction of a hydrogen atom by $\text{CO}_3^{\cdot-}$ from a carbon atom not involved in the π conjugation system of the corrin occurs in the first step, resulting in formation of a Co^{III} C-centered radical that undergoes rapid intramolecular electron transfer to form the corresponding Co^{II} carbocation complex for about 50% of these complexes. Subsequent competing pathways lead to formation of corrinoid complexes with two fewer hydrogen atoms and lactone derivatives of B₁₂. Our results demonstrate the potential of UHPLC combined with HRMS in the separation and identification of tetrapyrrole macrocycles with minor modifications from their parent molecule.

Introduction

Reactive oxygen and nitrogen species (ROS/RNS) are involved in numerous physiological and pathological processes, including cellular defense mechanisms, signal transduction, maintenance of cellular redox homeostasis, gene expression, and apoptosis.^[1] ROS/RNS include free radicals such as nitric oxide (NO), superoxide ($\text{O}_2^{\cdot-}$), the hydroxyl radical (OH), nitrogen dioxide (NO_2), and strong oxidizing and/or nitrating agents such as peroxynitrite/peroxynitrous acid ($\text{ONOO}(\text{H})$), hydrogen peroxide, and alkyl peroxide species (ROO , ROOH). The imbalance between the intracellular production of ROS/RNS and cellular defense mechanisms to destroy these species results in elevated ROS/RNS levels, which is known as oxidative stress. Exces-

sive ROS/RNS levels are associated with numerous diseases including cardiovascular disease, cancer, neurological diseases, and aging in general.^[2]

The carbonic acid/carbon dioxide plus water equilibrium [Eq. (1)] plays a crucial role in maintaining physiological pH conditions in mammals, with carbon dioxide being present in human tissues at millimolar concentrations.^[3]



As a consequence of this equilibrium, the role of the related radical, the carbonate radical anion ($\text{CO}_3^{\cdot-}$), in human disease and toxicology has become an area of considerable interest.^[4] As part of the immune response, activated macrophages produce high concentrations of NO and $\text{O}_2^{\cdot-}$, which react at almost diffusion-controlled rates to generate $\text{ONOO}(\text{H})$.^[5] $\text{CO}_3^{\cdot-}$ is generated from homolytic cleavage of the peroxo bond of the nitrosoperoxy carbonate anion ($\text{ONOOCO}_2^{\cdot-}$), the species formed from the reaction of ONOO^- with CO_2 .^[4,6] It has also been proposed that $\text{CO}_3^{\cdot-}$ is an intermediate formed from one-electron oxidation of HCO_3^- at the active site of Cu, Zn-superoxide dismutase and xanthine oxidase.^[7]

$\text{CO}_3^{\cdot-}$ is a strong one-electron oxidant ($E(\text{CO}_3^{\cdot-}, \text{H}^+/\text{HCO}_3^-) = 1.78 \text{ V}$ at pH 7.00^[8] and 1.59 V at pH 12.50^[9]) with an absorbance maximum at 600 nm ($\epsilon_{600\text{nm}} = 1860 \text{ M}^{-1} \text{ cm}^{-1}$).^[10] $\text{CO}_3^{\cdot-}$ reacts readily with tyrosine, cysteine, tryptophan, and methio-

[a] R. S. Dassanayake, Dr. J. T. Shelley
Department of Chemistry & Biochemistry
Kent State University, Kent, OH 44240 (USA)

[b] Dr. D. E. Cabelli
Department of Chemistry
Brookhaven National Laboratory, Upton, NY 11973 (USA)
E-mail: cabelli@bnl.gov

[c] Dr. N. E. Brasch
School of Applied Sciences, Auckland University of Technology
Private Bag 92006, Auckland 1142 (New Zealand)
E-mail: nbrasch@aut.ac.nz

Supporting information for this article is available on the WWW under <http://dx.doi.org/10.1002/chem.201406269>.

nine residues of proteins, and guanine residues of DNA and RNA.^[4,7,11] Studies on the reactivity of $\text{CO}_3^{\cdot-}$ with transition metal complexes,^[12] Mn porphyrins,^[13] and heme proteins^[3,14] have also been reported. $\text{CO}_3^{\cdot-}$ oxidizes reduced metal centers,^[14a-c] abstracts one or more hydrogen atoms from the ligand, and/or reacts with amino acid side chains of proteins leading to formation of radical complexes.^[3,14a,c,d]

Vitamin B₁₂ derivatives, also known as cobalamins (Cbls), Figure 1, are essential cofactors for mammalian methionine synthase and mitochondrial methylmalonyl-CoA mutase.^[15]

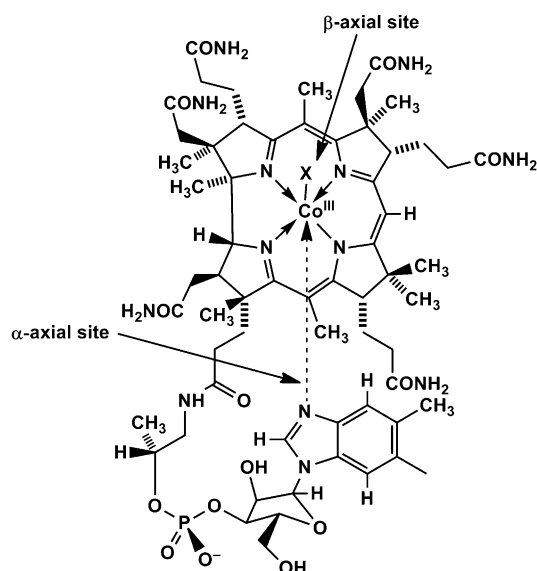


Figure 1. Labeling scheme for cobalamins. X = Me, 5'-deoxyadenosyl (Ado), H₂O, OH, CN, NO etc.

Like porphyrins, the metal center of reduced cobalamins is rapidly oxidized by ROS/RNS, including superoxide,^[16,17] nitric oxide,^[18] peroxynitrite,^[19] nitrogen dioxide,^[20] and nitrite.^[21] Furthermore ROS such as NO inactivate methionine synthase and methylmalonyl-CoA mutase.^[22] However, cell studies also show that vitamin B₁₂ derivatives protect against superoxide and hydrogen peroxide - induced intracellular oxidative stress,^[16,23] suggesting a potential role of cobalamin as a ROS/RNS scavenger for at least some of these ROS/RNS.

An important consideration is whether ROS/RNS damage the corrin ring of the cobalamin in addition to oxidizing the metal center of the reduced cobalamin forms. In this study pulse radiolysis has been utilized to investigate the reactions of the carbonate radical anion with cob(II)alamin and cob(III)alamin. The metal center of cob(II)alamin is rapidly oxidized by $\text{CO}_3^{\cdot-}$ to cob(III)alamin. Ultra-high-performance liquid chromatography combined with high-resolution mass spectrometry analysis has been successfully applied for the first time to analyze the complex mixture of corrinoid products that are obtained upon exposing cob(III)alamin to $\text{CO}_3^{\cdot-}$.

Results and Discussion

The reaction between cob(II)alamin (Cbl(II)) and $\text{CO}_3^{\cdot-}$

The reaction between $\text{CO}_3^{\cdot-}$ and the reduced vitamin B₁₂ derivative, cob(II)alamin, was studied by pulse radiolysis. The Cbl(II) concentration was kept at least five times higher than the $\text{CO}_3^{\cdot-}$ concentration, to achieve essentially pseudo-first order conditions. Self-recombination of $\text{CO}_3^{\cdot-}$ ($k = (4.3 \pm 0.4) \times 10^6 \text{ M}^{-1} \text{ s}^{-1}$ ^[24]) was unimportant in the time frame of the kinetic measurements. Figure 2 shows a plot of absorbance at 355 nm

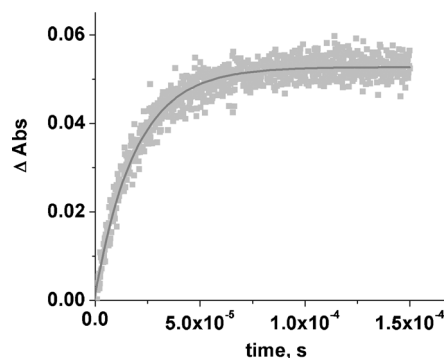


Figure 2. Change in absorbance at 355 nm versus time for the reaction of $\text{CO}_3^{\cdot-}$ ($1.6 \times 10^{-6} \text{ M}$) with excess Cbl(II) ($2.4 \times 10^{-5} \text{ M}$) at pH 9.00 (0.080 M KHCO_3 , 0.040 M KH_2PO_4 , RT, $l = 0.20 \text{ m}$, N_2O -saturated buffer). The best fit of the data to a first-order rate equation is superimposed on the data, giving $k_{\text{obs}} = (4.8 \pm 0.2) \times 10^4 \text{ s}^{-1}$.

versus time for the reaction between Cbl(II) ($2.4 \times 10^{-5} \text{ M}$) and $\text{CO}_3^{\cdot-}$ ($1.6 \times 10^{-6} \text{ M}$) at pH 9.00. The data in Figure 2 fit well to a first-order rate equation, with an observed first-order rate constant, $k_{\text{obs}} = (4.8 \pm 0.2) \times 10^4 \text{ s}^{-1}$. The rate constant is the same within experimental error when data are collected at 435 nm ($k_{\text{obs}} = (4.8 \pm 0.2) \times 10^4 \text{ s}^{-1}$; Figure S1, Supporting Information). Interestingly, k_{obs} for the reaction between Cbl(II) and $\text{CO}_3^{\cdot-}$ decreased slightly upon repetitive pulsing of the same solution. It was subsequently shown that $\text{CO}_3^{\cdot-}$ reacts with the reaction product (Cbl(III)=HOCbl), which may explain this observation. Hence data were collected with freshly prepared solutions for each measurement.

Rate constants for the reaction between Cbl(II) and $\text{CO}_3^{\cdot-}$ were also determined at other Cbl(II) concentrations at pH 9.00 and the data are summarized in Figure 3. The data fit well to a straight line passing through the origin, consistent with a single irreversible reaction. The linear relationship suggests that the reaction is first-order with respect to Cbl(II). From the slope, the apparent second-order rate constant (k_{app}) of the reaction was $(2.0 \pm 0.1) \times 10^9 \text{ M}^{-1} \text{ s}^{-1}$.

The pH dependence of the reaction was also investigated. Rate constants were determined at pH 10.52 and 11.50 at a range of Cbl(II) concentrations and the corresponding plots of k_{obs} versus [Cbl(II)] once again allowed the determination of k_{app} values (Figures S2 and S3, Supporting Information). Within experimental error, k_{app} is independent of pH ($(2.0 \pm 0.1) \times 10^9 \text{ M}^{-1} \text{ s}^{-1}$ from pH 9.00–11.50 (Table S1, Supporting Informa-

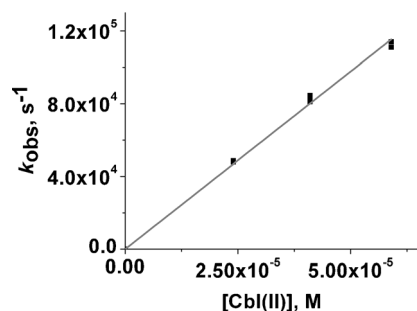


Figure 3. Observed pseudo first-order rate, k_{obs} , versus Cbl(II) concentration for the reaction between excess Cbl(II) ($(2.4\text{--}6.0) \times 10^{-5}$ M) and CO_3^{2-} ($(1.6\text{--}10.3) \times 10^{-6}$ M) at pH 9.00 (0.040 M KH_2PO_4 , 0.080 M KHCO_3 , $I=0.20$ M, RT, N_2O -saturated solutions). Data have been fitted with a line passing through origin, giving $k_{\text{app}} = (2.0 \pm 0.1) \times 10^9 \text{ M}^{-1} \text{ s}^{-1}$.

tion). Note that it was not possible to conduct experiments at pH values below 9.00 at the same HCO_3^- concentration, since the roughly 50 times lower reactivity of OH^\bullet with HCO_3^- ($k = 8.5 \times 10^6 \text{ M}^{-1} \text{ s}^{-1}$; $pK_a(\text{HCO}_3^-) \text{ ca. } 10^{[14d]}$) compared to OH^\bullet with CO_3^{2-} ($k = 3.9 \times 10^8 \text{ M}^{-1} \text{ s}^{-1}$ [14d]) results in incomplete scavenging of OH^\bullet by the carbonate buffer.

It is well established that Cbl(II) is oxidized to aquacobalamin/hydroxycobalamin ($\text{H}_2\text{OCbl}^+/\text{HOCbl}$; $pK_a(\text{H}_2\text{OCbl}^+) = 7.8^{[25]}$) in air.^[16a] In order to determine whether Cbl(II) is also oxidized to HOCbl by CO_3^{2-} , the change in absorbance with time was measured at different wavelengths for the reaction of Cbl(II) with CO_3^{2-} . The pulse radiolysis data were converted from absorbance to molar extinction coefficient values by assuming that one CO_3^{2-} oxidizes one Cbl(II) to HOCbl. This plot was compared with the change in molar extinction coefficient upon oxidizing Cbl(II) to HOCbl at pH 9.00, Figure 4. It is important to note that it was not possible to obtain full spectra as a function of time from our experimental setup for the pulse radiolysis experiments. There is excellent agreement between the two sets of data and the isosbestic wavelengths observed

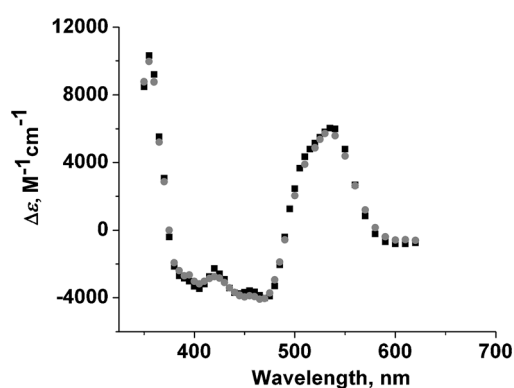


Figure 4. Change in molar extinction coefficient versus wavelength for the reaction of (■) Cbl(II) (4.5×10^{-5} M) with CO_3^{2-} ($(2.0\text{--}13.5) \times 10^{-6}$ M; produced by pulse radiolysis) at pH 9.00 (0.080 M KHCO_3 , 0.040 M KH_2PO_4 , RT, $I=0.20$ M, N_2O -saturated solution) and (●) Cbl(II) (6.5×10^{-5} M) exposed to O_2 (from air), to form HOCbl (pH 9.00, 0.080 M KHCO_3 , 0.040 M KH_2PO_4 , RT, $I=0.20$ M). The last values were calculated by converting absorbance values to molar extinction coefficients by dividing by the total Cbl concentration and subtracting one spectrum from the other.

at 375, 490, and 578 nm correspond to the expected values reported for the Cbl(II)/HOCbl conversion.^[19b] A similar result was also obtained at pH 10.52 (Figure S4, Supporting Information); hence under the pH conditions of our study CO_3^{2-} oxidizes Cbl(II) to Cbl(III) (HOCbl).

The stoichiometry of the reaction between Cbl(II) and CO_3^{2-} was investigated through the aid of a ^{60}Co γ -source to generate $\text{CO}_3^{\bullet -}$. Figure 5 shows UV/Vis spectroscopy data in which

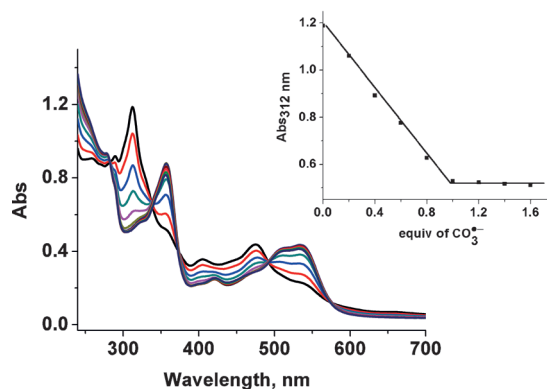


Figure 5. UV/Vis spectra for equilibrated solutions of Cbl(II) (4.0×10^{-5} M) with 0–2.0 mol equiv $\text{CO}_3^{\bullet -}$ at pH 11.50 (0.058 M KH_2PO_4 , 0.040 M KHCO_3 , $I=0.20$ M, RT, N_2O -saturated solution). Inset: Plot of absorbance at 312 nm versus mol equiv of $\text{CO}_3^{\bullet -}$.

a Cbl(II) sample (4.0×10^{-5} M) was repeatedly exposed to a continuous flux of $\text{CO}_3^{\bullet -}$ ($2.5 \times 10^{-7} \text{ M CO}_3^{\bullet -} \text{ s}^{-1}$) at 32 s time intervals (0–2 mol equiv $\text{CO}_3^{\bullet -}$ added in total) and UV/Vis absorption spectra recorded. Cbl(II) is oxidized to HOCbl ($\lambda_{\text{max}} = 358, 418, \text{ and } 535 \text{ nm}$) with sharp isosbestic points observed at 337, 374, 490, and 575 nm, in agreement with literature values for the Cbl(II)/HOCbl conversion.^[19b] The inset to Figure 5 gives a plot of absorbance at 312 nm as a function of mol equiv of $\text{CO}_3^{\bullet -}$ added for the same data. The absorbance at 312 nm decreased linearly up to 1.0 mol equiv $\text{CO}_3^{\bullet -}$ and is unchanged upon the addition of further $\text{CO}_3^{\bullet -}$ up to 1.4 mol equiv $\text{CO}_3^{\bullet -}$. From this data it is clear that the complete oxidation of Cbl(II) to Cbl(III) was observed after the addition of 1.0 mol equiv $\text{CO}_3^{\bullet -}$.

The product solution of the reaction between Cbl(II) and 1.0 mol equiv $\text{CO}_3^{\bullet -}$ (pH 11.50) was also analyzed by HPLC, once again confirming the formation of a single reaction product, HOCbl, Figure S5 in the Supporting Information. (Note that HOCbl is converted to H_2OCbl^+ under the mildly acidic conditions of the HPLC experiment.) Very small amounts (<2% by area at 350 nm) of unknown corrinoid species were also present, Figure S5 in the Supporting Information.

Our data suggest that the reaction between Cbl(II) and $\text{CO}_3^{\bullet -}$ proceeds according to Equation (2), with clean oxidation of the metal center of Cbl(II) to give HOCbl.



The second-order rate constant of $(2.0 \pm 0.1) \times 10^9 \text{ M}^{-1} \text{ s}^{-1}$ is of a comparable magnitude to the rate constants reported for the oxidation of the Fe^{II} center of heme proteins to Fe^{III} by

$\text{CO}_3^{\cdot-}$ ($0.057\text{--}1.1 \times 10^9 \text{ M}^{-1} \text{ s}^{-1}$ [14]), the oxidation of Mn^{II} porphyrins to Mn^{III} by $\text{CO}_3^{\cdot-}$ ($(1\text{--}5) \times 10^9 \text{ M}^{-1} \text{ s}^{-1}$ [13]) and the oxidation of Mn^{III} porphyrins to Mn^{IV} by $\text{CO}_3^{\cdot-}$ ($(0.27\text{--}5.4) \times 10^9 \text{ M}^{-1} \text{ s}^{-1}$ [13]). A single reaction was observed for the oxidation of Mn^{II} and Mn^{III} porphyrins by $\text{CO}_3^{\cdot-}$. [13] For heme proteins it has been proposed that $\text{CO}_3^{\cdot-}$ either initially abstracts a hydrogen atom to generate a protein radical intermediate, which subsequently oxidizes the Fe^{2+} center through intra- and intermolecular pathways, [14a,b,d] or that $\text{CO}_3^{\cdot-}$ directly oxidizes the reduced metal center. [14a,b] For the reaction between $\text{Cbl}(\text{II})$ and $\text{CO}_3^{\cdot-}$ it is most likely that the reaction involves direct oxidation of the metal center by $\text{CO}_3^{\cdot-}$. This is consistent with the 1:1 stoichiometry, the observation that a 1:1 stoichiometry was not observed in the reaction between $\text{Cbl}(\text{III})$ and $\text{CO}_3^{\cdot-}$, and UHPLC/HRMS data showing that $\text{CO}_3^{\cdot-}$ can abstract multiple hydrogen atoms from the periphery of the corrin ring of $\text{Cbl}(\text{III})$ (Table S2, Supporting Information).

Upon the addition of further $\text{CO}_3^{\cdot-}$ (> 1.4 mol equiv $\text{CO}_3^{\cdot-}$) to $\text{Cbl}(\text{II})$, additional small changes are observed in the UV/Vis spectrum (Figure S6, Supporting Information). These findings suggest that the HOCl produced in the reaction also reacts with $\text{CO}_3^{\cdot-}$, despite the metal center of HOCl already existing in the highest obtainable oxidation state (Co^{III}). Therefore, separate experiments were carried out to investigate this system.

The reaction between hydroxycobalamin (HOCl) and $\text{CO}_3^{\cdot-}$

The reaction of $\text{CO}_3^{\cdot-}$ with the Co^{III} vitamin B_{12} complex hydroxycobalamin was studied by pulse radiolysis under analogous conditions to the $\text{Cbl}(\text{II}) + \text{CO}_3^{\cdot-}$ experiments, at pH 9.00, 10.52, and 11.50. Figure 6 shows the change in absorbance at 530 nm over time for the reaction of $\text{CO}_3^{\cdot-}$ ($1.5 \times 10^{-6} \text{ M}$) with excess HOCl ($4.0 \times 10^{-5} \text{ M}$) at pH 11.50. From these data it is clear that two major reactions are observed. The best fit of the data to two consecutive irreversible first-order reactions is superimposed on the data, giving $k_{1\text{obs}} = (2.2 \pm 0.1) \times 10^4 \text{ s}^{-1}$ and $k_{2\text{obs}} = (3.6 \pm 0.2) \times 10^3 \text{ s}^{-1}$. The rate constants are essentially the same when data were collected at 390 nm ($k_{1\text{obs}} = (2.2 \pm 0.1) \times$

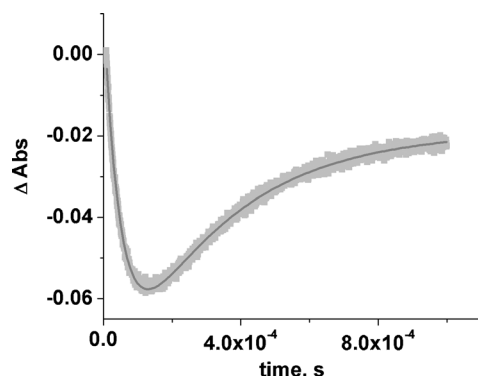


Figure 6. Plot of change in absorbance at 530 nm versus time for the reaction of $\text{CO}_3^{\cdot-}$ ($1.5 \times 10^{-6} \text{ M}$) with excess HOCl ($4.0 \times 10^{-5} \text{ M}$) at pH 11.50 (0.040 M KHCO_3 , $0.058 \text{ M KH}_2\text{PO}_4$, $I = 0.20 \text{ M}$, RT). The best fit of the data to two consecutive first-order reactions is superimposed on the data, giving $k_{1\text{obs}} = (2.2 \pm 0.1) \times 10^4 \text{ s}^{-1}$ and $k_{2\text{obs}} = (3.6 \pm 0.2) \times 10^3 \text{ s}^{-1}$.

10^4 s^{-1} and $k_{2\text{obs}} = (3.4 \pm 0.2) \times 10^3 \text{ s}^{-1}$; Figure S7, Supporting Information).

Rate data were subsequently collected over a range of HOCl concentrations, keeping the HOCl concentration in excess ($(4.0\text{--}20) \times 10^{-5} \text{ M}$) compared with the $\text{CO}_3^{\cdot-}$ concentration. Figure 7 shows the plot of observed rate constant ($k_{1\text{obs}}$)

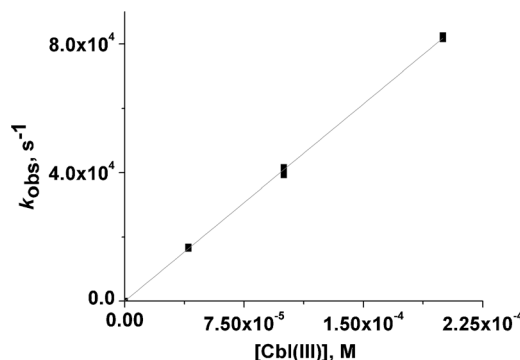


Figure 7. Observed rate constant, $k_{1\text{obs}}$, versus HOCl concentration for the initial reaction between HOCl ($(4.0\text{--}20.0) \times 10^{-5} \text{ M}$) and $\text{CO}_3^{\cdot-}$ ($(1.6\text{--}25.0) \times 10^{-6} \text{ M}$) at pH 11.50 ($0.058 \text{ M KH}_2\text{PO}_4$, 0.040 M KHCO_3 , $I = 0.20 \text{ M}$, RT, N_2O -saturated solution). Data have been fitted to a line passing through origin, giving $k_{1\text{app}} = (4.5 \pm 0.2) \times 10^8 \text{ M}^{-1} \text{ s}^{-1}$.

for the first reaction of $\text{Cbl}(\text{III})$ with $\text{CO}_3^{\cdot-}$ as a function of $\text{Cbl}(\text{III})$ concentration at pH 11.50 ($0.040 \text{ M KH}_2\text{PO}_4$, 0.080 M KHCO_3 , $I = 0.20 \text{ M}$, RT, N_2O -saturated buffer). The data fit well to a straight line passing through the origin, consistent with a single irreversible reaction. The linear relationship suggests that the reaction is first-order with respect to the concentration of $\text{Cbl}(\text{III})$. From the slope, the apparent second-order rate constant of the reaction at this pH ($k_{1\text{app}}$) is $(4.5 \pm 0.2) \times 10^8 \text{ M}^{-1} \text{ s}^{-1}$.

Kinetic data were also collected over a range of HOCl concentrations at pH 9.00 and 10.52 (only for a single concentration of $\text{Cbl}(\text{III})$), giving $k_{1\text{app}} = (4.1 \pm 0.2) \times 10^8 \text{ M}^{-1} \text{ s}^{-1}$ (Figure S8, Supporting Information) and $(4.4 \pm 0.2) \times 10^8 \text{ M}^{-1} \text{ s}^{-1}$, respectively. Given the similarity in these rate constants to the value obtained at pH 11.50 ($(4.5 \pm 0.2) \times 10^8 \text{ M}^{-1} \text{ s}^{-1}$), $k_{1\text{app}}$ is independent of pH in this pH range. The data is summarized in Table 1. The observed rate constant for the second reaction, $k_{2\text{obs}}$, was found to be essentially independent of the HOCl concentration at pH 11.52 (see Table 1).

Table 1. Apparent second-order rate constants ($k_{1\text{app}}$) and observed first-order rate constants ($k_{2\text{obs}}$) for the reaction of HOCl with $\text{CO}_3^{\cdot-}$ as a function of pH (carbonate buffer, $I = 0.20 \text{ M}$, RT, N_2O -saturated solution). Errors in individual values are estimated to be about 10%.

pH ± 0.02	$10^4 [\text{HOCl}]$ [M]	$10^5 [\text{CO}_3^{\cdot-}]$ [M]	$10^{-8} k_{1\text{app}}$ [$\text{M}^{-1} \text{ s}^{-1}$]	$10^{-3} k_{2\text{obs}}$ [s^{-1}] ^[a]
9.00	0.4–2.0	0.3–1.2	4.1	1.8
10.52	0.5	0.3–2.5	4.4 ^[b]	3.3
11.50	0.5–2.5	0.3–3.0	4.5	3.5

[a] Mean value of 3–9 data points. [b] Reported rate constant is based on a single data point.

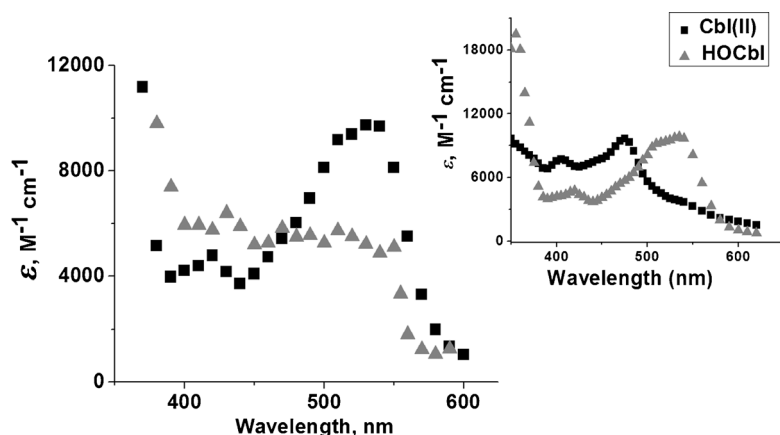


Figure 8. Plot of extinction coefficient versus wavelength for the reaction of HOCbl (4.0×10^{-5} M) with $\text{CO}_3^{\bullet-}$ ($(1.5-7.5) \times 10^{-6}$ M) at pH 11.50 (0.058 M KH_2PO_4 , 0.040 M KHCO_3 , $I=0.20$ M, RT, N_2O -saturated solution) (▲) intermediate and (■) final product. Inset: Molar extinction coefficients of (▲) HOCbl and (■) Cbl(II).

Figure 8 shows the absorbance spectra of the intermediate and the product(s) generated from the pulse radiolysis data, for which the molar extinction coefficients, calculated assuming a mechanism in which one carbonate radical is converted to the first intermediate and that the intermediate is converted to the second intermediate, are used to facilitate better comparison with known spectra (Figure 8 inset). The absorption spectrum of the intermediate was obtained by the addition of extinction coefficients of the HOCbl to the extinction coefficient of the intermediate to accommodate for the loss of starting material in the pulse. An analogous procedure was carried out to calculate the extinction coefficient of the product. The inset of Figure 8 shows UV/Vis absorption spectra of HOCbl and Cbl(II) for comparison purposes. Within the limitations of the experimental set up, the spectrum of the intermediate is not typical for either Cbl(II) or HOCbl (Co^{II} corrinoids are blue shifted compared with Co^{III} corrinoids), but instead resembles an approximately equal mixture of both. The spectrum of the product solution is similar to that expected for a Co^{III} corrinoid and is remarkably similar to the starting complex, HOCbl. Similar spectral changes were also observed for data collected at pH 10.52 (Figure S9, Supporting Information).

The stoichiometry of the reaction between HOCbl and $\text{CO}_3^{\bullet-}$ was also investigated utilizing a ^{60}Co source to generate $\text{CO}_3^{\bullet-}$ by means of γ radiolysis of water. Figure 9 shows UV/Vis spectroscopy data in which a single HOCbl sample (5.0×10^{-5} M) was exposed repeatedly to a $\text{CO}_3^{\bullet-}$ flux (2.5×10^{-7} M $\text{CO}_3^{\bullet-} \text{ s}^{-1}$) for 40 s time periods (0–2.0 mol equiv $\text{CO}_3^{\bullet-}$ added) and UV/Vis spectra recorded. The most notable point here is that there is a relatively small spectral change. From Figure 9 it is clear that the absorbance at 350 and 550 nm decreases, whereas the absorbance at 460 nm increases as the mol equiv of $\text{CO}_3^{\bullet-}$ increases. The isosbestic points observed at 334, 383, 491, and 594 nm are not consistent with conversion between HOCbl/Cbl(II) (337, 374, 490, and 574 nm).^[19b] The inset to Figure 9 gives a plot of absorbance at 358 nm versus mol equiv of $\text{CO}_3^{\bullet-}$ generated from the same data. The absorbance at 358 nm decreases linearly upon the addition of up to 2.0 mol

equiv $\text{CO}_3^{\bullet-}$. The absorbance change was considerably smaller than that observed for the reaction between Cbl(II) and $\text{CO}_3^{\bullet-}$, Figure 5. Specifically, the absorbance change at 358 nm for the reaction of HOCbl with 1.0 mol equiv $\text{CO}_3^{\bullet-}$ is about 10% of that observed for the Cbl(II)/HOCbl conversion. Importantly, after the addition of 2.0 mol equiv $\text{CO}_3^{\bullet-}$, no significant spectral change was observed after exposing the final product solution to air, consistent with the final product(s) being corrin ring-modified Co^{III} corrinoid complexes rather than

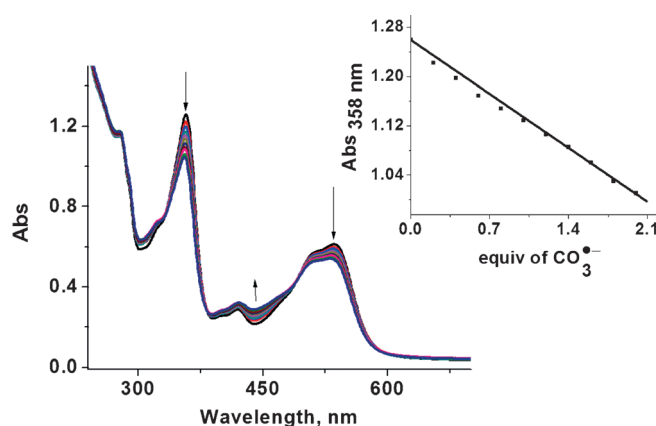


Figure 9. UV/Vis spectra for equilibrated solutions of HOCbl (5.0×10^{-5} M) with 0–2.0 mol equiv $\text{CO}_3^{\bullet-}$ at pH 11.50 (0.058 M KH_2PO_4 , 0.040 M KHCO_3 , $I=0.20$ M, RT, N_2O -saturated solution). Inset: Plot of absorbance at 358 nm versus mol equiv of $\text{CO}_3^{\bullet-}$.

the product solution containing air-sensitive Co^{II} corrinoid complexes. This is consistent with the plots of molar extinction coefficient versus wavelength for this product solution versus HOCbl, which are indistinguishable from each other (Figure S10, Supporting Information).

To further investigate the nature of the corrinoid product(s) of the reaction between HOCbl and $\text{CO}_3^{\bullet-}$, a sample of HOCbl (8.0×10^{-5} M) exposed to 1.0 mol equiv $\text{CO}_3^{\bullet-}$ at pH 9.00 (0.040 M KH_2PO_4 , 0.080 M KHCO_3 , $I=0.20$ M, RT, N_2O -saturated buffer) was analyzed by ultra-high-performance liquid chromatography combined with high-resolution mass spectrometry (UHPLC/HRMS; mass accuracies better than 0.0008 Da). Note that peak separation was not achievable using conventional HPLC. The Van de Graaff pulse radiolysis set up was used to generate $\text{CO}_3^{\bullet-}$ through the radiolysis of water. From the UV/Vis absorption chromatogram and the extracted ion signal chromatogram in the mass range of doubly charged corrinoid product species (m/z 640–690), Figure 10, it is apparent that numerous complexes are formed. Analysis of the peaks by MS

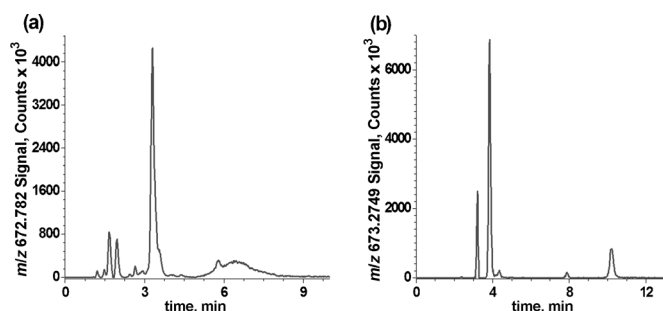


Figure 10. Plot of extracted ion signal in the m/z 640–690 range versus time for the product solution formed from the reaction between HOCbl (8.0×10^{-5} M) with 1.0 mol equiv $\text{CO}_3^{\cdot-}$ at pH 9.00 (0.040 M KH_2PO_4 , 0.080 M KHCO_3 , $I = 0.20$ M, RT, N_2O -saturated buffer). Inset: Corresponding UV/Vis chromatogram of the product solution at 350 nm.

shows that the carbonate radical abstracts hydrogen atoms from multiple sites on the corrin ring, and lactone derivatives are also formed, see Table S2 in the Supporting Information. Specifically, seven peaks can be assigned to corrinoids with two hydrogen atoms abstracted from the corrin ring (Cbl–2H) and four peaks can be assigned to corrinoids with four fewer hydrogen atoms than cobalamin (Cbl–4H). Numerous peaks were assignable to lactone derivatives of B_{12} and lactone complexes minus two hydrogen atoms. Four peaks correspond to B_{12} derivatives incorporating two lactone modifications. Figure 11 gives ion signal chromatograms for $m/z = 672.783$ ($[(\text{H}_2\text{OCbl}-2\text{H}) + \text{H}]^{2+}$) and $m/z = 673.275$ (lactone derivatives of

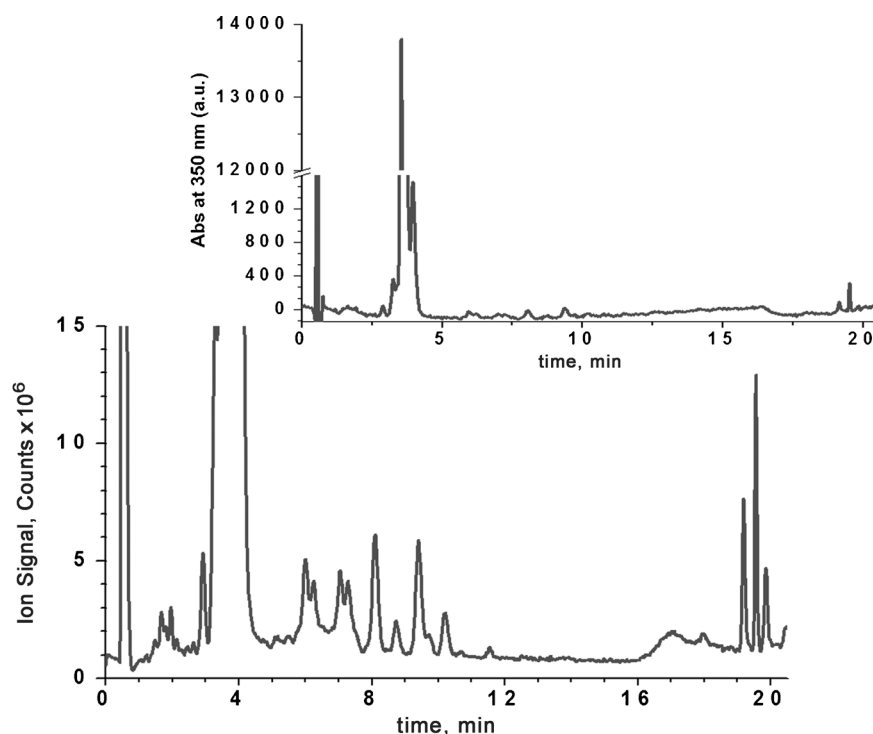


Figure 11. Plot of extracted ion signal for a) $m/z = 672.783$ (corresponding to the doubly charged Cbl–2H complex, and b) $m/z = 673.275$ (lactone derivative of B_{12}) versus time for the products of the reaction of HOCbl (8.0×10^{-5} M) with 1.0 mol equiv $\text{CO}_3^{\cdot-}$ at pH 9.00 (0.040 M KH_2PO_4 , 0.080 M KHCO_3 , $I = 0.20$ M, RT, N_2O -saturated buffer).

$[\text{H}_2\text{OCbl}]^+$). A typical mass spectrum for one of the peaks of the UV/Vis chromatogram and the corresponding mass spectrum simulation is shown in Figure S11, Supporting Information. The c-lactone derivative of B_{12} is well-known, Figure 12,^[26] with a UV/Vis spectrum that is similar to the parent B_{12} complex.^[27] Note that our experimental data does not tell us at which ring positions lactone formation occurs nor the position at which two or four hydrogen atoms are abstracted. Unmodified Cbl reactant was observed at 3.67 min.

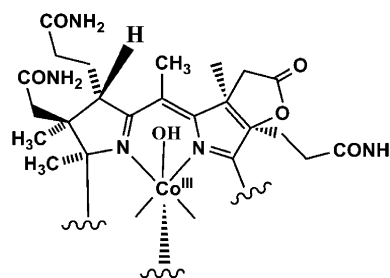


Figure 12. Structure of the c-lactone analogue of B_{12} .

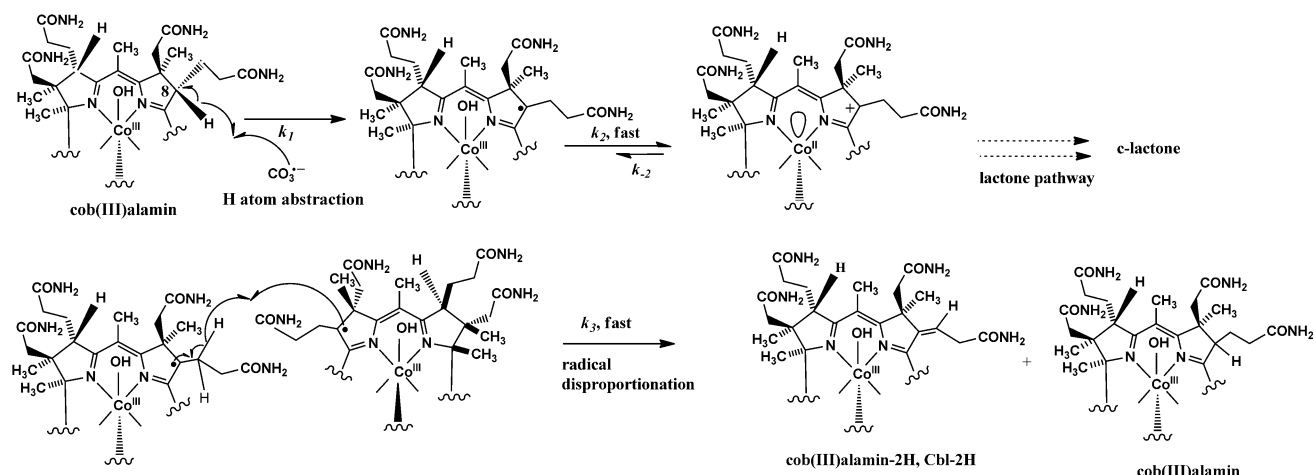
The products of the reaction of HOCbl (1.0×10^{-3} M) with 1.0 mol equiv $\text{CO}_3^{\cdot-}$ (pH 9.00, 0.040 M KH_2PO_4 , 0.080 M KHCO_3 , $I = 0.20$ M, RT, N_2O -saturated buffer) generated by radiolysis of water utilizing a ^{60}Co source was also analyzed by UHPLC/HRMS. A comparison of the ion signal chromatogram with the ion signal chromatogram using the Van de Graaff to generate $\text{CO}_3^{\cdot-}$ is given in Figure S12 in the Supporting Information. Using the Van der Graff radiation source, the entire amount of $\text{CO}_3^{\cdot-}$ is generated within 3 μs prior to the onset of the second observed reaction, whereas for the ^{60}Co experiments, a steady state flux of $\text{CO}_3^{\cdot-}$ is produced over an extended time period. Given this difference, the chromatograms are remarkably similar, and once again mass spectral evidence was produced for formation of Cbl–2H, Cbl–4H, Cbl, lactones, lactones–2H and B_{12} derivatives incorporating two lactones upon exposure of HOCbl to $\text{CO}_3^{\cdot-}$. Peak assignments for the ^{60}Co data are given in Table S3, Supporting Information.

The UHPLC/HRMS was also recorded for commercial HOCbl-HCl at pH 9.00 (0.040 M KH_2PO_4 , 0.080 M KHCO_3 , $I = 0.20$ M, RT; see Figure S13, Sup-

porting Information). The main peak at 3.66 min can be assigned to $[\text{Cbl}+\text{H}]^{2+}$ rather than the parent $[(\text{H}_2\text{OCbl})+\text{H}]^{2+}$ complex, indicating that H_2OCbl^+ is reduced to $\text{Cbl}(\text{II})^+$, which undergoes a one-electron oxidation ($\text{Cbl}(\text{II})^+ \rightarrow \text{Cbl}(\text{II})^{2+}$) by the ESI source to form $\text{Cbl}(\text{II})^+$. Others have shown that ESI sources can oxidize or reduce parent molecules.^[28] The intensity of the $[\text{Cbl}+\text{H}]^{2+}$ ion in the mass spectrum was significantly weaker for CNCbl due to the presence of the strong π -acceptor CN^- ligand versus the weaker H_2O ligand at the β -axial site (CNCbl UHPLC/HRMS data not shown). Peak assignments are given in the Supporting Information, Table S4. Interestingly, the low-signal peaks observed at 2.77, 3.34 and 3.46 min correspond to $\text{Cbl}-2\text{H}$ complexes. A weak peak corresponding to the lactone was also observed at 10.53 min. Note that the signals associated with all of these species are significantly greater for the product mixture of $\text{Cbl}(\text{III}) + 1.0$ mol equiv CO_3^{2-} ; hence in this latter case these species arise as a consequence of reactions between $\text{Cbl}(\text{III})$ and CO_3^{2-} , rather than only as impurities in the commercially obtained $\text{Cbl}(\text{III})$ reactant. Observing these impurities so clearly in the Cbl reactant highlights the sensitivity of our UHPLC/HRMS set up versus a conventional LC-MS instrument.

A further interesting feature of the UHPLC/HRMS of the $\text{Cbl}(\text{III}) + 1.0$ mol equiv CO_3^{2-} product mixture was the observation of an isomer of cobalamin at about 4.0 min retention time (Tables S2 and S3 in the Supporting Information), regardless of the method used to generate CO_3^{2-} , which was present only in freshly diluted samples of the product solution. (This species was not observed for authentic $\text{Cbl}(\text{III})$, nor the product solutions that had been diluted in water or buffer several days earlier.) One possible site for isomerization is at $\text{C}_{13}-\text{C}_{15}$, Scheme S1, Supporting Information. Two diastereoisomers are possible, since hydrogen atoms can add to the radical from both sides of the corrin ring. It is not clear to us why the isomer is unstable in dilute solutions.

Reaction pathways observed in the kinetic experiments have been proposed, Scheme 1, based on several key experimental observations:

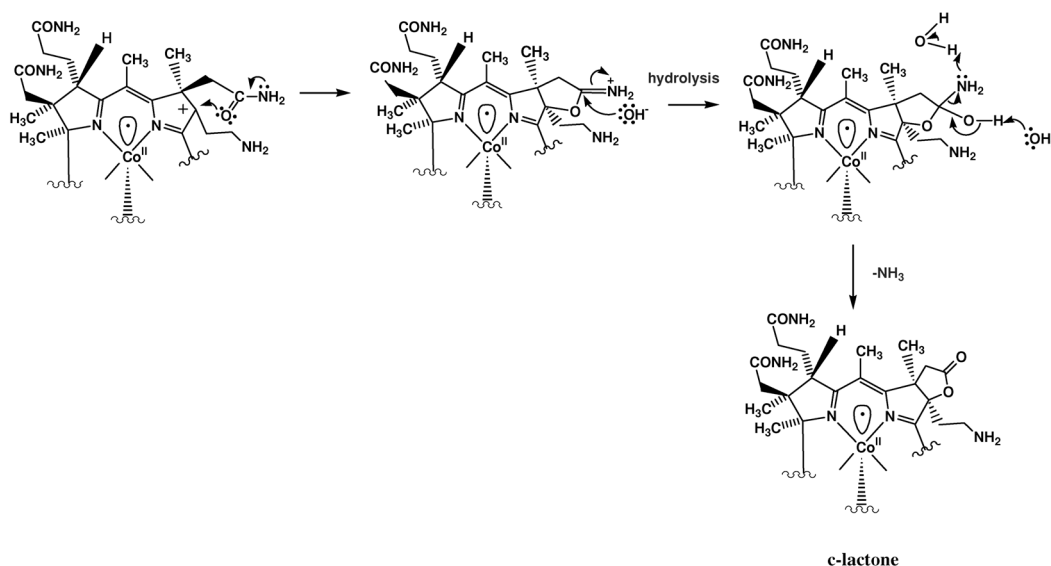


Scheme 1. Proposed reaction pathways for the reaction of excess $\text{Cbl}(\text{III})$ (HOCbl) with CO_3^{2-} . Abstraction of a hydrogen atom by CO_3^{2-} can occur at multiple sites in addition to C_8 (shown).

- 1) In the kinetic experiments with the $\text{Cbl}(\text{III})$ concentration in excess, the first observed reaction was first-order with respect to $\text{Cbl}(\text{III})$, whereas the rate of the second reaction was independent of the initial concentration of $\text{Cbl}(\text{III})$.
- 2) Both reactions are independent of pH in the pH range of this study.
- 3) A 1:1 $\text{HOCbl}:\text{CO}_3^{2-}$ stoichiometry was not observed and the products are predominately if not solely Co^{II} complexes.
- 4) The absorbance changes for the first observed reaction in the kinetic experiments are consistent with approximately half the reaction intermediates being Co^{II} complexes.
- 5) UHPLC/HRMS evidence was found for the formation of corrinoid species that have two or four fewer hydrogen atoms than $\text{Cbl}(\text{III})$ and lactone derivatives of B_{12} .

The rate of abstraction of hydrogen atoms by CO_3^{2-} would be expected to be dependent on the HOCbl concentration, consistent with the HOCbl concentration dependence of the first observed reaction. In Scheme 1 abstraction of a hydrogen atom from the C_8 position of the corrin ring is shown. Abstracting hydrogen atoms from carbons involved in the corrin ring π system results in blue shift of the spectrum to give characteristic spectra for "stable yellow corrinoids";^[29] hence, since the UV/Vis spectrum of the product mixture is so similar to the reactant HOCbl , this does not occur to any significant extent for our system. Four other likely positions where hydrogen atoms are initially abstracted from HOCbl are the C_3 , C_{13} , C_{18} and C_{19} carbon atoms of the corrin ring (see Figure 1), resulting in formation of multiple corrin radical intermediates.^[27,29,30] The rate constant k_1 is therefore a macroscopic value corresponding to hydrogen abstraction by CO_3^{2-} at multiple sites. Hydrogen atoms can be subsequently added from either side of the corrin ring, leading to diastereoisomers.

The absorbance changes for the first observed reaction in the kinetic studies indicate that approximately half the reaction intermediates are Co^{II} complexes. This finding suggests that under the experimental conditions of this study a rapid intramolecular electron transfer to the Co center of the corrin



Scheme 2. Proposed reaction pathway for formation of lactone derivatives of B₁₂ (c-lactone formation shown).

occurs for about 50% of the C-centered Co^{III} radicals (k_2 , Scheme 1), with $k_2 \gg k_1$. The abstraction by a C-centered radical of a hydrogen atom from the solvent (H₂O) is slow (k ca. 10^4 – 10^6 M⁻¹ s⁻¹ [31]); hence this reaction is unlikely to occur. Experiments in which H₂O was replaced with D₂O showed that the reaction rates of both observed reactions are the same regardless of H₂O or D₂O being the solvent (k_{HIE} ca. 1, see Figure S14, Supporting Information); therefore abstraction of a hydrogen atom from the C-centered radical by solvent is not a rate-determining step. Furthermore the reaction rate was independent of the HCO₃⁻ or H₂PO₄⁻ concentration (additional experiments carried out at 0.20 M carbonate buffer in the absence of phosphate at pH 9.00); hence these species are also not involved in a rate-determining step (data not shown).

The most plausible mechanism by which a complex minus two hydrogen atoms is formed is by means of abstraction of a hydrogen atom from the C-centered radical by another C-centered radical, Scheme 1 (disproportionation—although this is only strictly correct if the two C-centered radicals are identical, which is unlikely to be the case, since there are multiple sites where hydrogen atom abstraction by CO₃⁻ may occur). This leads to formation of a complex with two fewer hydrogen atoms than Cbl(III) and the original Cbl(III) complex if the hydrogen atom adds to the same side of the corrin, Scheme 1. This is consistent with the observation that the UV/Vis spectrum of the product is very similar to the Cbl(III) reactant, since abstraction of two hydrogen atoms from carbon atoms not involved in the π conjugation system will have little effect on the UV/Vis spectrum. Radical disproportionation reactions for carbon-centered radicals are well-known and are extremely rapid (10^8 – 10^{10} M⁻¹ s⁻¹). [31,32] Given that the oxidation state of the Co and the corrin ring conjugation is not altered in this last reaction, this reaction is not observable in the kinetic experiments. The second observed reaction, which is independ-

ent of the initial Cbl(III) concentration and pH, is assigned to the conversion of the Co^{II} complexes back to Co^{III} C-centered radicals (k_{-2}).

Importantly, UHPLC/HRMS characterization of the product mixture of the kinetic and ⁶⁰Co experiments showed that multiple lactone complexes are formed in addition to Cbl–2H complexes. A mechanism has been proposed for lactone formation under the conditions of the kinetic experiments (CO₃⁻ consumed in the first step of the reaction), Scheme 2. Under the conditions of the ⁶⁰Co experiments in which a constant flux of CO₃⁻ is generated, it is likely that all Co^{II} complexes are instead rapidly oxidized to their corresponding Co^{III} forms, given that the reaction between Cbl(II) and CO₃⁻ is so rapid ($k=2.0 \times 10^9$ M⁻¹ s⁻¹, preceding section). Lactone formation (five-membered rings) can occur subsequent to hydrogen atom abstraction by CO₃⁻ from C3, C8, C13, and C19, with two possible lactones formed at C3 and C8. Under the conditions used for the ⁶⁰Co experiments (higher mol equiv CO₃⁻) it is also possible that CO₃⁻ abstracts a second hydrogen atom from the C-centered Co^{III} radical to generate Cbl–2H, in addition to rapid oxidation of the Co^{II} carbocation to form the corresponding Co^{III} complex, which reacts further to form a lactone.

The change in the molar extinction coefficients for the first observed reaction were found to decrease as the CO₃⁻ radical concentration increases. For example, the change in the molar extinction coefficient, $\Delta\epsilon$, for the reaction between Cbl(III) (80 μ M) and carbonate (2.8 μ M) at 530 nm was about 6100 M⁻¹ cm⁻¹ (pH 9.00, 0.20 M KHCO₃, RT), whereas $\Delta\epsilon$ for the reaction between Cbl(III) (80 μ M) and carbonate (78 μ M) at 530 nm was about 3300 M⁻¹ cm⁻¹ under the same experimental conditions. This suggests that in the latter case only approximately 50% of the carbonate radical reacts with Cbl(III) to give Cbl(III)/Co^{III}, whereas the remaining CO₃⁻ reacts with the C-centered radical to abstract a second hydrogen atom and/or

oxidizes one or more of the Co^{II} radical intermediates, since the oxidation of a $\text{Cbl}(\text{II})$ by $\text{CO}_3^{\cdot-}$ is about five times faster (see above). Finally, it is worth noting that although complete separation of the species was not possible using conventional HPLC, the ES-MS of the fractions supports the UHPLC/HRMS results; specifically evidence was also found for formation of multiple $\text{Cbl}-2\text{H}$ species and lactones. The formation of lactone complex(es) was also supported by the FT-IR spectrum of an HPLC fraction of the product mixture, which exhibited a peak at 1772 cm^{-1} ($\text{C}=\text{O}$ stretch), Figure S15, Supporting Information.

Others have reported that reacting Fe^{III} heme proteins with $\text{CO}_3^{\cdot-}$ does not indirectly lead to reduction of the metal center.^[3,14a,c] Rate constants for hydrogen atom abstraction by $\text{CO}_3^{\cdot-}$ in the range of 4.7×10^7 – $3.7 \times 10^9\text{ M}^{-1}\text{ s}^{-1}$ have been reported for these reactions.^[3,14a,c] However, the indirect reduction of Fe^{III} heme proteins by the hydroxyl radical via a heme radical intermediate has been reported.^[14d,33] The subsequent transfer of the unpaired electron to the metal center has been proposed to occur by means of intramolecular and electron-tunneling mechanisms.^[33c] To our knowledge, rates of intramolecular electron transfer from the periphery of the corrin or porphyrin to the metal center have not been reported. The rate constant for the intramolecular reduction of a Fe^{III} heme protein radical to Fe^{II} is $\lesssim 10^5\text{ s}^{-1}$.^[33e]

Conclusions

The rate constant of the reaction between $\text{Cbl}(\text{II})$ and $\text{CO}_3^{\cdot-}$ has been directly determined using pulse radiolysis and was found to be $2.0 \times 10^9\text{ M}^{-1}\text{ s}^{-1}$ (pH 9.00–11.50). $\text{Cbl}(\text{II})$ is cleanly oxidized to HOCbl . The reaction of $\text{CO}_3^{\cdot-}$ with HOCbl proceeds in two steps. The rate constant for the initial abstraction of a hydrogen atom from the corrin ring by $\text{CO}_3^{\cdot-}$ is $4.3 \times 10^8\text{ M}^{-1}\text{ s}^{-1}$ (pH 9.00–11.50), which is five times slower than the rate constant for the $\text{Cbl}(\text{II}) + \text{CO}_3^{\cdot-}$ reaction. The observed rate constant for the second reaction is about $3.0 \times 10^3\text{ s}^{-1}$ and is independent of the initial $\text{Cbl}(\text{III})$ concentration. We propose that $\text{CO}_3^{\cdot-}$ abstracts hydrogen atoms from multiple carbon atoms not involved in the π conjugation system, resulting in formation of a Co^{III} C-centered radical complex, which undergoes rapid intramolecular transfer of the unpaired electron to the metal center for about 50% of these complexes. The second observed step is assigned to conversion of the Co^{II} radical complex back to the C-centered radical complex, which rapidly combines with a second C-centered radical to form the starting material and a $\text{Cbl}-2\text{H}$ complex. UHPLC/HRMS studies of the products of the reaction between $\text{Cbl}(\text{III})$ and 1.0 mol equiv $\text{CO}_3^{\cdot-}$ also provide evidence for formation of multiple lactone derivatives. Our results highlight the potential of UHPLC/HRMS to separate and characterize corrinoids with minor structural modifications. It is likely that this extremely sensitive combined technique will also be very valuable in the assessment of complex product mixtures of the closely related porphyrin systems.

Experimental Section

Materials and methods

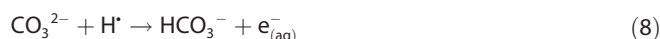
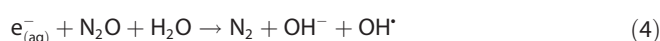
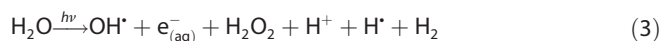
Chemicals: Hydroxycobalamin hydrochloride, $\text{HOCbl}\cdot\text{HCl}\cdot n\text{H}_2\text{O}$ ($\geq 96\%$, 10–15% water, batch dependent^[34]) was purchased from Fluka and sodium borohydride ($\geq 98\%$) and acetic acid were obtained from Acros Organics. Potassium dihydrogen phosphate, sodium hydroxide, ammonia, acetonitrile (HPLC grade), absolute methanol (LC/MS grade), water (HPLC grade) and potassium cyanide ($\geq 99\%$) were purchased from Fisher Scientific. Potassium bicarbonate ($\geq 99\%$), sodium hydrogen phosphate ($\geq 99\%$), potassium hydroxide and sodium hydroxide were obtained from J.T. Baker Chemical Company. Water was purified with a Barnstead Nanopure Diamond or Millipore water purification systems.

Synthesis of Cob(II)alamin (Cbl(II)): $\text{Cbl}(\text{II})$ (ca. 96% pure) was synthesized using a previously described procedure.^[16a]

Determination of Cbl concentrations: Cbl concentrations were determined by converting Cbls to dicyanocobalamin, $(\text{CN})_2\text{Cbl}^-$. Cobalamins were allowed to react with KCN (0.10 M, pH 11.50) to produce $(\text{CN})_2\text{Cbl}^-$ ($\epsilon_{368\text{ nm}} = 30\,000\text{ M}^{-1}\text{ cm}^{-1}$ ^[35]).

pH measurements: pH measurements were carried out at room temperature using an Orion model 520 A or 710 A pH meter equipped with Mettler-Toledo Inlab 423 or 421 pH electrodes. The electrode was filled with a 3 M KCl/saturated AgCl solution (pH 7.0) and standardized with standard buffer solutions at pH 9.00, 10.52, 11.50. Solution pH was adjusted using H_3PO_4 , NaOH, or KOH solutions as necessary.

Pulse radiolysis experiments: Pulse radiolysis studies were carried out at Brookhaven National Laboratory with a 2 MeV Van de Graaff accelerator producing electron pulses (pulse width 30–300 ns) that resulted in about $(1\text{--}30) \times 10^{-6}\text{ M}$ primary radicals generated in aqueous solution. $\text{CO}_3^{\cdot-}$ was generated upon irradiation of N_2O -saturated aqueous solutions containing 0.080 M carbonate buffer at pH 9.00 and 0.040 M carbonate buffer at pH 10.52 and pH 11.50 by means of the reactions given in Equations (3)–(8).^[13] Irradiating water generates $\cdot\text{OH}$, e_{aq}^- and $\cdot\text{H}$, and in N_2O -saturated aqueous solutions containing $\text{HCO}_3^-/\text{CO}_3^{2-}$ these primary radicals are rapidly converted to $\text{CO}_3^{\cdot-}$.^[14c]



An aqueous potassium thiocyanate solution (0.010 M) saturated with N_2O (0.026 M) was used for radiation dosimetry, taking $G(\text{SCN})_2^{\cdot-} = 6.13$, in which G is the number of moles formed per $1.602 \times 10^{-17}\text{ J}$ of energy absorbed by the solution, and $\epsilon_{472\text{ nm}} = (7590 \pm 230)\text{ M}^{-1}\text{ cm}^{-1}$.^[36] The optical path of the cell was 2 cm. Solid $\text{Cbl}(\text{II})$ or $\text{HOCbl}\cdot\text{HCl}$ was added to the appropriate carbonate buffer in the solution reservoir that had been rendered anaerobic by bubbling Ar for about 15 min and the solution was then degassed for a further 15 min. The solution was subsequently saturated with N_2O for about 5 min prior to collecting data. Reported rate constants are average values of at least three independent meas-

urements at three different wavelengths. The data were collected and fitted using the Numerical Integration of Chemical Kinetics program in PRWIN (by H. Schwarz, BNL). Note that the error of each measurement is estimated to be about 10%.

^{60}Co γ -radiolysis studies on the reaction of cob(II)alamin and cob(III)alamin with carbonate radicals at pH 11.50: A phosphate buffer solution (pH 11.50; 0.058 M KH_2PO_4 , 0.040 M KHCO_3 , $I=0.20$, 25.00 mL) was saturated with N_2O gas for 10–15 min. Cbl(II) (ca. 1.77 mg) solid was quickly added and the solution bubbled for a further 2–3 min. The solution was transferred to a N_2O -flushed quartz cuvette, capped and the cuvette repeatedly exposed to a ^{60}Co radiation source (ca. $2.5 \times 10^{-7} \text{ M CO}_3^{\cdot-} \text{ s}^{-1}$) at a fixed distance for 40 s time intervals. The UV/Vis spectrum was subsequently recorded after each irradiation. A similar experiment was carried out replacing Cbl(II) with HOCbl-HCl (pH 11.50; 0.058 M KH_2PO_4 , 0.040 M KHCO_3 , $I=0.20$, RT).

UV/Vis experiments: Anaerobic UV/Vis spectrometric measurements were carried out using either a Cary 5 (RT measurements) or a Cary 5000 spectrophotometer equipped with a thermostated ($25.0 \pm 0.1^\circ\text{C}$) cell changer operating with WinUV Bio software (version 3.00). Data were fitted using the program Microcal Origin version 8.0.

High-performance liquid chromatography (HPLC) experiments: HPLC analyses were carried out with an Agilent 1100 series HPLC system equipped with a degasser, quaternary pump, autosampler, and a photodiode array detector (resolution of 2 nm), using an Alltech Alltima C_{18} semipreparative column (5 μm , 100 \AA , 10 mm \times 300 mm) thermostated to 25°C . A mobile phase consisting of acetate buffer (1% v/v CH_3COOH , pH 3.5), **A**, and CH_3CN (1% v/v CH_3COOH), **B**, were used with the following method: 0–18 min isocratic elution of 92.5:7.5 **A/B**, 18–20 min 92.5:7.5 to 50:50 **A/B**, 20–25 min isocratic elution of 50:50 **A/B**, 25–28 min 50:50 to 92.5:7.5 **A/B**. All gradients were linear and a flow rate of 2 mL min^{-1} was used. Product peaks were monitored at 254 and 350 nm.

Ultra-high performance liquid chromatography (UHPLC) experiments: UHPLC analyses were carried out using a Dionex Ultimate 3000 rapid separation liquid chromatograph equipped with a degasser, quaternary pump, autosampler, and a photodiode array detector (bandwidth of 2 nm). Analytes were separated on a Thermo Scientific Hypersil GOLD C_{18} column (1.9 μm , 175 \AA , 2.1 mm \times 55 mm). The following multistep gradient method with acetate buffer (1% v/v CH_3COOH , pH 3.5), **A**, and CH_3OH , **B**, was used to separate constituents: 0–15 min 90:10 to 86:14 **A/B**, 15–20 min 86:14 to 65:35 **A/B**, 20–21 min 65:35 to 50:50 **A/B**, 21–26 min isocratic elution of 50:50 (column rinse), 26–27 min 50:50 to 90:10 **A/B**, 27–30 min isocratic column conditioning at 90:10 **A/B**. All gradients were linear and maintained at a flow rate of $0.300 \text{ mL min}^{-1}$. Product peaks were monitored at 254 and 350 nm with a reference wavelength of 398 nm. Eluent from the separation was directly infused into the electrospray ionization source of the mass spectrometer, described below.

High-resolution mass spectrometry (HRMS) measurements: High resolution mass spectra of the eluting species were obtained using an Exactive Plus mass spectrometer (Thermo Scientific, Bremen, Germany) equipped with a heated electrospray ionization source (HESI II probe, Thermo Scientific, Bremen, Germany). The source was operated at 3.5 kV with a sheath gas flow rate and gas heater temperature of 25 (manufacturers units) and 310°C , respectively, to cope with the relatively high liquid flow rates. Mass spectra were recorded in the positive ionization mode with a scan range of 133–2000 m/z , a mass resolving power setting of 140,000, and an automatic gain control (AGC) target value of 1×10^6 ions. To ensure very high mass accuracy ($>0.75 \text{ mmu}$), the instrument was

calibrated daily and a lock mass of m/z 371.10124, due to polysiloxane, was used throughout. These settings resulted in a spectral acquisition rate of ~ 1.9 spectra/second. All UV absorption and mass spectral data were collected and processed with the Xcalibur software (ver. 3.0, Thermo Scientific, San Jose, CA, USA).

Acknowledgements

The authors gratefully acknowledge the assistance of Dr. Donald L. Dick (Department of Chemistry, Colorado State University, CO, USA) and Dr. Mahinda Gangoda (KSU) with mass spectrometry and FT-IR experiments. This research was funded by the US National Institute of General Medical Sciences of the National Institutes of Health under award number 1R15M094707-01A1. The content is solely the responsibility of the authors and does not necessarily represent the official views of the National Institutes of Health. The work at Brookhaven National lab was carried out at the Accelerator Center for Energy Research, which is supported by the U.S. DOE Office of Science, Division of Chemical Sciences, Geosciences and Biosciences under Contract No. DE-AC02-98CH10886.

Keywords: carbonate radical • cobalamins • kinetics • pulse radiolysis • vitamin B_{12}

- [1] a) B. G. David, *J. Phys. D* **2012**, *45*, 415305; b) P. D. Ray, B. W. Huang, Y. Tsuji, *Cell. Signalling* **2012**, *24*, 981–990.
- [2] a) M. Valko, D. Leibfritz, J. Moncol, M. T. D. Cronin, M. Mazur, J. Telser, *Int. J. Biochem. Cell Biol.* **2007**, *39*, 44–84; b) V. Chiurchiu, M. Maccarrone, *Antioxid. Redox Signaling* **2011**, *15*, 2605–2641.
- [3] L. Gebicka, J. Didik, J. Gebicki, *Res. Chem. Intermed.* **2009**, *35*, 401–409.
- [4] O. Augusto, M. G. Bonini, A. M. Amanso, E. Linares, C. C. X. Santos, S. L. L. De Menezes, *Free Radical Biol. Med.* **2002**, *32*, 841–859.
- [5] S. V. Lyman, J. K. Hurst, *J. Am. Chem. Soc.* **1995**, *117*, 8867–8868.
- [6] M. G. Bonini, R. Radi, G. Ferrer-Sueta, A. M. D. C. Ferreira, O. Augusto, *J. Biol. Chem.* **1999**, *274*, 10802–10806.
- [7] D. B. Medinas, G. Cerchiaro, D. F. Trindade, O. Augusto, *IUBMB Life* **2007**, *59*, 255–262.
- [8] M. G. Bonini, O. Augusto, *J. Biol. Chem.* **2001**, *276*, 9749–9754.
- [9] R. E. Huie, C. L. Clifton, P. Neta, *Int. J. Radiat. Appl. Instrum. C Radiat. Phys. Chem.* **1991**, *38*, 477–481.
- [10] J. L. Weeks, J. Rabani, *J. Phys. Chem.* **1966**, *70*, 2100–2106.
- [11] a) A. M. Fleming, C. J. Burrows, *Chem. Res. Toxicol.* **2013**, *26*, 593–607; b) C. Crean, Y. Uvaydov, N. E. Geacintov, V. Shafirovich, *Nucleic Acids Res.* **2008**, *36*, 742–755.
- [12] P. C. Mandal, D. K. Bardhan, S. N. Bhattacharyya, *J. Radioanal. Nucl. Chem.* **1995**, *191*, 349–359.
- [13] G. Ferrer-Sueta, D. Vitturi, I. Batinić-Haberle, I. Fridovich, S. Goldstein, G. Czapski, R. Radi, *J. Biol. Chem.* **2003**, *278*, 27432–27438.
- [14] a) F. Boccini, A. S. Domazou, S. Herold, *J. Phys. Chem. A* **2004**, *108*, 5800–5805; b) F. Boccini, A. S. Domazou, S. Herold, *J. Phys. Chem. A* **2006**, *110*, 3927–3932; c) A. S. Domazou, W. H. Koppenol, *J. Biol. Inorg. Chem.* **2007**, *12*, 118–125; d) S. Goldstein, A. Samuni, *Free Radical Biol. Med.* **2005**, *39*, 511–519.
- [15] a) L. Randaccio, S. Geremia, N. Demitri, J. Wuerges, *Molecules* **2010**, *15*, 3228–3259; b) R. Banerjee, *Chemistry and Biochemistry of B12*, Wiley, New York, **1999**, pp. 1–800.
- [16] a) E. Suarez-Moreira, J. Yun, C. S. Birch, J. H. H. Williams, A. McCaddon, N. E. Brasch, *J. Am. Chem. Soc.* **2009**, *131*, 15078–15079; b) E. S. Moreira, N. E. Brasch, J. Yun, *Free Radical Biol. Med.* **2011**, *51*, 876–883.
- [17] R. S. Dassanayake, D. E. Cabelli, N. E. Brasch, *ChemBioChem* **2013**, *14*, 1081–1083.
- [18] K. E. Broderick, V. Singh, S. Zhuang, A. Kambo, J. C. Chen, V. S. Sharma, R. B. Pilz, G. R. Boss, *J. Biol. Chem.* **2005**, *280*, 8678–8685.

- [19] a) R. Mukherjee, N. E. Brasch, *Chem. Eur. J.* **2011**, *17*, 11723–11727; b) R. Mukherjee, N. E. Brasch, *Chem. Eur. J.* **2011**, *17*, 11805–11812.
- [20] R. S. Dassanayake, D. E. Cabelli, N. E. Brasch, *J. Inorg. Biochem.* **2015**, *142*, 54–58.
- [21] N. T. Plymale, R. S. Dassanayake, H. A. Hassanin, N. E. Brasch, *Eur. J. Inorg. Chem.* **2012**, 913–921.
- [22] a) I. O. Danishpajoo, T. Gudi, Y. Chen, V. G. Kharitonov, V. S. Sharma, G. R. Boss, *J. Biol. Chem.* **2001**, *276*, 27296–27303; b) A. Kambo, V. S. Sharma, D. E. Casteel, V. L. Woods, R. B. Pilz, G. R. Boss, *J. Biol. Chem.* **2005**, *280*, 10073–10082.
- [23] C. S. Birch, N. E. Brasch, A. McCaddon, J. H. H. Williams, *Free Radical Biol. Med.* **2009**, *47*, 184–188.
- [24] K. S. Haygarth, T. W. Marin, I. Janik, K. Kanjana, C. M. Stanisky, D. M. Bartels, *J. Phys. Chem. A* **2010**, *114*, 2142–2150.
- [25] L. Xia, A. G. Cregan, L. A. Berben, N. E. Brasch, *Inorg. Chem.* **2004**, *43*, 6848–6857.
- [26] a) D. L. Anton, H. P. C. Hogenkamp, T. E. Walker, N. A. Matwiyoff, *J. Am. Chem. Soc.* **1980**, *102*, 2215–2219; b) R. Bonnett, *Chem. Rev.* **1963**, *63*, 573–605; c) R. Bonnett, J. M. Godfrey, V. B. Math, P. M. Scopes, R. N. Thomas, *J. Chem. Soc. Perkin Trans. 1* **1973**, 252–257; d) A. Gossauer, B. Grüning, L. Ernst, W. Becker, W. S. Sheldrick, *Angew. Chem. Int. Ed. Engl.* **1977**, *16*, 481–482; *Angew. Chem.* **1977**, *89*, 486–487; e) B. Grüning, G. Holze, T. A. Jenny, P. Nesvadba, A. Gossauer, L. Ernst, W. S. Sheldrick, *Helv. Chim. Acta* **1985**, *68*, 1754–1770; f) K. ó Proinsias, M. Giedyk, D. Gryko, *Chem. Soc. Rev.* **2013**, *42*, 6605–6619.
- [27] R. Bonnett, J. R. Cannon, A. W. Johnson, A. Todd, *J. Chem. Soc.* **1957**, 1148–1158.
- [28] a) V. Kertesz, G. Van Berkel, *J. Solid State Electrochem.* **2005**, *9*, 390–397; b) D. Rondeau, F. Rogalewicz, G. Ohanessian, E. Levillain, F. Odobel, P. Richomme, *J. Mass Spectrom.* **2005**, *40*, 628–635; c) R. Vessecchi, Z. Naal, J. N. C. Lopes, S. E. Galembek, N. P. Lopes, *J. Phys. Chem. A* **2011**, *115*, 5453–5460; d) N. B. Cech, C. G. Enke, *Mass Spectrom. Rev.* **2001**, *20*, 362–387.
- [29] J. M. Pratt, *Inorganic Chemistry of Vitamin B12*, Academic Press, London, New York, **1972**, pp. 1–295.
- [30] S. Y. S. Ing, J. J. Pfiffner, *Arch. Biochem. Biophys.* **1968**, *128*, 281–284.
- [31] P. Neta, P. Grodkowski, A. B. Ross, *J. Phys. Chem. Ref. Data* **1996**, *25*, 709–1050.
- [32] S. W. Benson, *J. Phys. Chem.* **1985**, *89*, 4366–4369.
- [33] a) J. R. Clement, N. T. Lee, M. H. Klapper, L. M. Dorfman, *J. Biol. Chem.* **1976**, *251*, 2077–2082; b) N. N. Lichtin, A. Shafferman, G. Stein, *Biochim. Biophys. Acta* **1974**, *357*, 386–398; c) J. W. Van Leeuwen, A. Raap, W. H. Koppenol, H. Nauta, *Biochim. Biophys. Acta Bioenerg.* **1978**, *503*, 1–9; d) J. W. Van Leeuwen, J. Tromp, H. Nauta, *Biochim. Biophys. Acta* **1979**, *577*, 394–399; e) K. D. Whitburn, J. J. Shieh, R. M. Sellers, M. Z. Hoffman, I. A. Taub, *J. Biol. Chem.* **1982**, *257*, 1860–1869.
- [34] N. E. Brasch, R. G. Finke, *J. Inorg. Biochem.* **1999**, *73*, 215–219.
- [35] H. A. Barker, R. D. Smyth, H. Weissbach, J. I. Toohey, J. N. Ladd, B. E. Volcani, *J. Biol. Chem.* **1960**, *235*, 480–488.
- [36] D. E. Polyansky, D. Cabelli, J. T. Muckerman, T. Fukushima, K. Tanaka, E. Fujita, *Inorg. Chem.* **2008**, *47*, 3958–3968.

Received: November 28, 2014

Published online on March 11, 2015